

Scalar Field Dominated Cosmology with Woods-Saxon Like Potential

Sreerag Radhakrishnan^{1*}, Sarath Nelleri^{2†} and Navaneeth Poonthottathil^{2‡}

¹Department of Physics, Government Brennen College, Dharmadam, Thalassery 670106, India

²Department of Physics, Indian Institute of Technology, Kanpur-208016, India

Abstract

Dark energy can be characterized by a canonical scalar field, known as quintessence. Quintessence allows for a dynamical equation of state $-1 \leq \omega \leq -\frac{1}{3}$. In this work, we consider a quintessence model with a specific potential of the Woods-Saxon form. The model is studied at late phase assuming flat cosmology, and the model parameters are constrained using Type Ia supernova data and Observational Hubble data. In particular we employ Markov Chain Monte Carlo methods for the Bayesian inference of these parameters. We obtain the value of the Hubble constant $H_0 = 68.10 \pm 0.74 \text{ kms}^{-1} \text{ Mpc}^{-1}$ and the matter energy density parameter $\Omega_{m_0} = 0.31 \pm 0.01$, which are consistent with the values obtained using base Λ CDM using the same dataset. Computation of the χ^2_{min} , AIC and BIC reveal that this model is preferred according to AIC and χ^2_{min} criteria, while the Λ CDM is preferred according to BIC. We also show that this model can explain late-time accelerated expansion. Statefinder analysis reveals a Chaplygin gas behaviour in the past, in addition to the quintessence behaviour of the field.

1 Introduction

Contemporary cosmology attempts to unmask the mystery of dark energy, which drives the (observed) late-time accelerated expansion of the Universe. The initial evidence for this was from the observations of Type Ia Supernovae (SNeIa) as presented in Ref. [1, 2], which confirmed the acceleration of the Universe. According to such observations, the Universe is assumed to be dominated by a mysterious component called dark energy, constituting about 70% of the present Universe, the rest consisting of matter, of which normal baryonic matter is only around 4%, and the remaining is in the form of "invisible" dark matter. This inference has also been confirmed by observations of the CMB [3, 4] and Baryonic Acoustic Oscillations [5, 6].

Dark energy is characterized by a perfect fluid with a negative equation of state, $\omega = P/\rho$. One of the simplest models for dark energy is the cosmological constant Λ . The cosmological constant has a characteristic equation of state $\omega = -1$. This is the currently accepted model of dark energy, by the standard Λ CDM. Physical explanation of the cosmological constant may be attributed to the zero-point quantum vacuum fluctuations in the Universe [7], given by $\Lambda = 8\pi G\rho_{vac}/c^2$. However, theoretical predictions of ρ_{vac} do not match with the current observations, by several orders of magnitude [8, 9]. This cosmological constant problem, suggests that the mentioned explanation for the cosmological constant is unsatisfactory. In addition to this, Λ CDM encounters problems such as the Cosmological Coincidence Problem [10] and the tensions in the inferred values of various parameters between low redshift data [11, 12, 13] and high redshift data [14, 15, 16]. Attempts to resolve these issues have been ongoing and many possible solutions have been suggested in the form of alternate cosmological models. These include the modified gravity models (Ref. [17, 18, 19, 20, 21]), which modify the curvature term

*sreeragradhakrishnan01@gmail.com

†sarathnelleri@gmail.com

‡navaneeth@iitk.ac.in

in Einstein Field Equations, and modified (or dynamical) dark energy models which modify the form of the energy-momentum tensor in the field equations [22, 23, 24, 25, 26, 27, 28, 29, 30, 31].

Such kinds of modified dark energy models characterize dark energy as a specific form of matter, such as quintessence [32], k-essence [33] or the Chaplygin gas [34]. The quintessence is a particular model in which a scalar field is slow rolling down a potential that is similar to that of early Universe inflation models [35]. Reviews of various quintessence models can be found in Ref. [36, 37, 38, 39, 40, 41, 42, 43, 44, 45, 46, 47]. Another kind of scalar field model is k-essence, which, unlike quintessence, does not have a canonical kinetic term. These models have also been studied extensively [48, 49, 50, 51, 52] much like quintessence. The advantage of these scalar field models is that some of these models can address the fine tuning and coincidence problem, all the while explaining the late-time cosmic acceleration. These models are distinguished by their dynamical equation of state ω , which is not the case for Λ CDM.

The evolution of ω is the key factor in distinguishing quintessence models. Quintessence can be of two broad types : (i) thawing models and (ii) freezing models. In thawing models, at early times, the field was frozen by Hubble damping at a value different from its minimum potential, started to roll down to the minimum at late times. These models have an early equation of state $\omega_\phi \approx -1$ and becomes less negative over time, that is, $\omega'_\phi > 0$. In the case of freezing models, the scalar field is already rolling towards its minimum potential, but slows down at later times when it dominates the Universe. This means that the equation of state "freezes" close to the present time and $\omega'_\phi < 0$.

The aim of this paper is to construct a quintessence model with a potential which has a similar form as that of the Woods-Saxon potential of nuclear physics. In Sec. 2, we present our proposed model, which will be referred to as the Woods-Saxon Quintessence or WSQ hereafter. It is essential to emphasize that while we draw inspiration from the form of the Woods-Saxon potential, this model is entirely distinct in its interpretation within the context of quintessence cosmology. In Sec. 3, we employ Bayesian inference to constrain the model parameters using observational data, specifically the Type Ia supernova data and observational Hubble parameter data. In Sec. 4, we investigate the evolution of various cosmological parameters within the framework of the WSQ model. Finally, we conclude our work in Sec. 5.

2 Woods-Saxon Quintessence

We consider a quintessence in the presence of non-relativistic matter, represented by a barotropic perfect fluid. As we are focusing on the late-time cosmology, the effect of radiation component is negligibly small and hence, we only consider the contribution from matter and field. The action would be given by

$$S = \int d^4x \sqrt{-g} \left[\frac{1}{2} \frac{R}{\kappa^2} - \frac{1}{2} g^{\mu\nu} \partial_\mu \phi \partial_\nu \phi - V(\phi) \right] + S_m, \quad (1)$$

where $\kappa^2 = 8\pi G$, S_m is the matter action, R is the Ricci scalar, $g^{\mu\nu}$ and g are the metric and its determinant respectively. Here, $V(\phi)$ is the potential over which the field ϕ is rolling towards some minima. We study the quintessence in the flat Friedmann-Lemaître-Robertson-Walker (FLRW) background with the curvature parameter $k = 0$. For a quintessence field ϕ , the pressure and energy density are given by $P_\phi = \frac{\dot{\phi}^2}{2} - V(\phi)$ and $\rho_\phi = \frac{\dot{\phi}^2}{2} + V(\phi)$ respectively, where the overdot represents derivative with respect to cosmic time t . Then, the equation of state takes the form

$$\omega_\phi = \frac{P_\phi}{\rho_\phi} = \frac{\frac{\dot{\phi}^2}{2} - V(\phi)}{\frac{\dot{\phi}^2}{2} + V(\phi)}. \quad (2)$$

Here, we assume that the dark matter and field are non-interacting and hence satisfies individual conservation equations

$$\dot{\rho}_\phi + 3H(\rho_\phi + P_\phi) = 0, \quad (3)$$

$$\dot{\rho}_m + 3H\rho_m = 0, \quad (4)$$

where the dark matter is assumed to be pressureless, giving an equation of state $\omega_m = 0$. Introducing the forms of ρ_ϕ and P_ϕ in Eq. (3), we obtain the Klein-Gordon equation,

$$\ddot{\phi} + 3H\dot{\phi} + V_{,\phi} = 0, \quad (5)$$

where $V_{,\phi} = \frac{dV}{d\phi}$ and $H = \frac{\dot{a}}{a}$ is the Hubble parameter. The Friedmann equations in this framework can be obtained as,

$$3H^2 = \kappa^2 \left[\frac{\dot{\phi}^2}{2} + V(\phi) + \rho_m \right], \quad (6)$$

$$2\dot{H} = -\kappa^2 [\dot{\phi}^2 + \rho_m]. \quad (7)$$

We consider a potential $V(\phi)$ which resembles the Woods-Saxon potential,

$$V(\phi) = \frac{2V_0}{e^{\kappa(\phi-\phi_0)} + 1}, \quad (8)$$

where V_0 and ϕ_0 are the values of the potential energy and scalar field at present time, i.e., at redshift $z = 0$, respectively. Analytical solution to Eq. (7) is challenging with the potential $V(\phi)$. In order to solve Eq. (7) numerically, we introduce three dimensionless parameters,

$$x = \frac{\dot{\phi}\kappa}{\sqrt{6}H_0}, \quad y = \frac{\sqrt{V(\phi)}\kappa}{\sqrt{3}H_0}, \quad h = \frac{H}{H_0}, \quad (9)$$

where H_0 is the Hubble parameter at present. Taking the derivatives of x , y and h with z and using Eq. (5), (6) and (7), we obtain three coupled differential equations,

$$\frac{dx}{dz} = \frac{3x}{1+z} - \sqrt{\frac{3}{2}} \frac{y^2}{h(1+z)} \left[1 - \frac{1}{2} \left(\frac{y}{y_0} \right)^2 \right], \quad (10)$$

$$\frac{dy}{dz} = \sqrt{\frac{3}{2}} \frac{xy}{h(1+z)} \left[1 - \frac{1}{2} \left(\frac{y}{y_0} \right)^2 \right], \quad (11)$$

$$\frac{dh}{dz} = \frac{3h^2 + x^2 - y^2}{2h(1+z)}. \quad (12)$$

Here we have defined $y_0 = y(z=0)$. On solving these equations numerically, we obtain x , y , and h as a function of z . These variables are related through the equation,

$$h^2 = x^2 + y^2 + \Omega_m, \quad (13)$$

where we have defined $\Omega_m = \rho_m/\rho_{c_0} = \rho_m\kappa^2/3H_0^2$, where $\rho_{c_0} = 3H_0^2/\kappa^2$ is the present value of the critical density. We define the energy density parameter of the field, Ω_ϕ using Eq. (9) in terms of the variables x and y as,

$$\Omega_\phi = \frac{\kappa^2\rho_\phi}{3H_0^2} = x^2 + y^2. \quad (14)$$

The equation of state can be written using Eq. (2) as,

$$\omega_\phi = \frac{x^2 - y^2}{x^2 + y^2}. \quad (15)$$

In this model, H_0 , Ω_{m_0} and Ω_{ϕ_0} are the physical quantities of interest that are to be determined. Our aim is to estimate these parameters utilizing the latest observational probes.

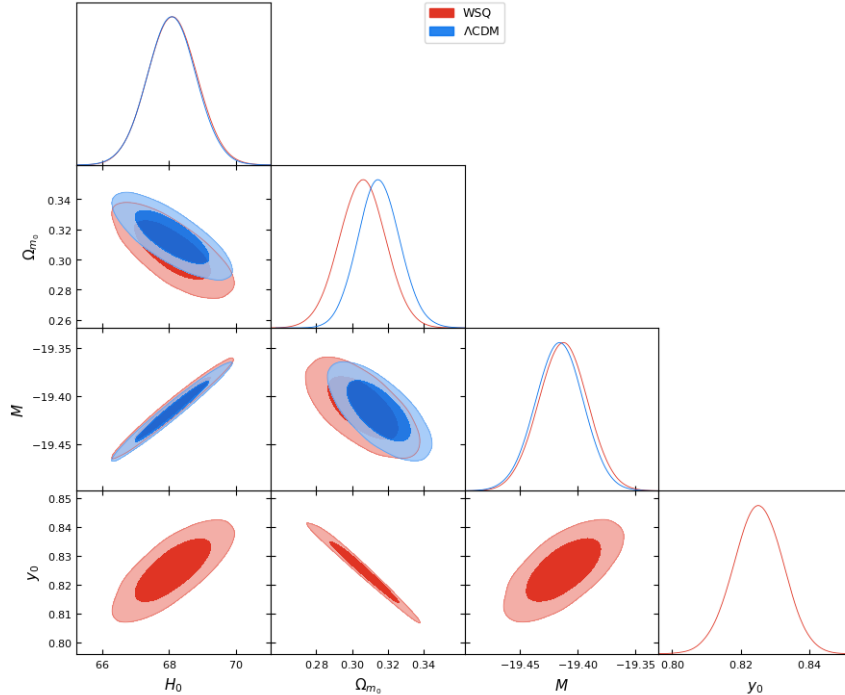


Figure 1: The 2D confidence contours for 68% and 95% probabilities and 1D posterior distribution of the model parameters using SNIa+OHD datasets for Λ CDM and the WSQ model. The chosen prior ranges are $40 \leq H_0 \leq 100$, $0 \leq \Omega_{m_0} \leq 1$, $-20 \leq M \leq -18$ and $-1 \leq y_0 \leq 1$

3 Data Analysis

In order to perform the data analysis, we have to solve the coupled differential equations presented in Eq. (10)-(12), which require the initial conditions x_0 , y_0 and h_0 . These parameters are constrained by the equation $1 = x_0^2 + y_0^2 + \Omega_{m_0}$, where $h_0 = 1$. Thus, the WSQ model has effectively three independent free parameters H_0 , Ω_{m_0} and y_0 . In order to constrain these parameters, we employ Markov Chain Monte Carlo methods for Bayesian inference [53]. The primary input for the Bayesian inference is the prior range for each model parameter. We assume a sufficiently large prior range for H_0 between 40 and 100, and 0 to 1 for Ω_{m_0} . The prior range for y_0 is assumed to be -1 to 1 as the present density parameters of the components add to unity. The parameters are constrained using Observational Hubble Data (OHD) and Type Ia Supernova (SNIa) data. The datasets we used are that from [54] for OHD and the Pantheon+ sample [55] for SNIa. The OHD dataset consists of 77 redshift vs Hubble parameter values in the redshift range $0 \leq z \leq 2.36$, obtained from cosmic chronometers, BAO signal in galaxy distribution and BAO signals in the $Ly\alpha$ forest distribution. The Pantheon+ data comprises the sample of 1701 Type Ia supernova light curves of 1550 distinct supernovae discovered in the redshift range $0 \leq z \leq 2.3$ [56]. The apparent magnitude of SNIa, m is obtained from the expression,

$$m(z) = 5 \log_{10} \left[\frac{d_L(z)}{Mpc} \right] + M + 25, \quad (16)$$

where M is the absolute magnitude of SNIa and d_L is the luminosity distance and for flat cosmology ($\Omega_k = 0$), it is given by,

$$d_L(z) = c(1+z) \int_0^z \frac{dz'}{H(z')}, \quad (17)$$

where c is the speed of light in vacuum expressed in km/s. The χ^2 value for OHD data is computed as,

$$\chi_{OHD}^2 = \sum_{i=1}^{77} \left[\frac{H_{obs}(z_i) - H_{th}(z_i, H_0, \Omega_{m_0}, y_0)}{\sigma(z_i)} \right]^2, \quad (18)$$

where H_{obs} and H_{th} are the values of Hubble parameter observed and that computed using the WSQ model respectively, and σ is the error in the measurement. The χ^2 for the SNIa Pantheon+ data is calculated using the expression,

$$\chi_{SNIa}^2 = \Delta \vec{D}^T C_{stat+syst}^{-1} \Delta \vec{D}, \quad (19)$$

where $\Delta \vec{D}$ is the vector of distance modulus residual given by,

$$\Delta \vec{D} = \mu(z_i) - \mu_{th}(z_i, H_0, \Omega_{m_0}, M, y_0), \quad (20)$$

and $C_{stat+syst}$ is the covariance matrix that includes both statistical and systematic covariances. Here, $\Delta \vec{D}^T$ refers to the transpose of $\Delta \vec{D}$. The distance modulus $\mu = m - M$. Then, the total χ^2 is obtained as,

$$\chi_{total}^2 = \chi_{OHD}^2 + \chi_{SNIa}^2. \quad (21)$$

The parameter set $(H_0, \Omega_{m_0}, M, y_0)$ that minimises the $\chi_{total}^2 = -2 \log_e(\mathcal{L})$, where \mathcal{L} is the Gaussian likelihood, is the best-fit parameters. We utilize the information criteria such as Akaike Information Criterion (AIC) and Bayesian Information Criterion (BIC) for the model comparison. We use the definitions of AIC and BIC as,

$$AIC = n \log_e \left(\frac{\chi^2}{n} \right) + 2k, \quad (22)$$

$$BIC = n \log_e \left(\frac{\chi^2}{n} \right) + k \log_e(n). \quad (23)$$

We used a well tested and open source PYTHON implementation of the affine-invariant ensemble sampler for MCMC proposed by Goodman and Weare called emcee for parameter inference. More details about emcee and its implementation can be found in Ref. [57, 58]. We also employed the multiprocessing module from PYTHON standard library and the numba module to reduce the computation time. The best-fit values of the model parameters are presented in Table 1 and the marginal likelihood of the model parameters are presented in Fig. 1. The minimum χ^2 obtained for the WSQ model with the SNIa + OHD dataset is $\chi_{min}^2 = 1813.94$ while for Λ CDM, we obtained $\chi_{min}^2 = 1818.39$. This suggests that the WSQ model is preferred over the Λ CDM according to the χ_{min}^2 criteria. A similar trend is

Data	SNIa + OHD
H_0	68.1041 ± 0.7374
Ω_{m_0}	0.3059 ± 0.0129
M	-19.4126 ± 0.0212
y_0	0.8251 ± 0.0072

Table 1: The best-fit model parameters of the WSQ model and its uncertainties within 1σ confidence

followed with the AIC value, with $\Delta AIC = 2.36$. However, BIC tends to penalize the extra parameter to a greater extent, so the Λ CDM is preferred over the WSQ model according to the ΔBIC criteria. The estimated value for the Hubble constant $H_0 = 68.10 \pm 0.74$, which is in close agreement with the Planck 2018 results [15]. The current value of the dark energy density parameter is computed as $\Omega_{\phi_0} = 0.6941 \pm 0.0129$. With the estimated parameters, we analyse the background evolution of cosmological parameters within the WSQ background.

Model	χ^2_{min}	AIC	BIC
Λ CDM	1818.3949	45.9428	62.3926
WSQ	1813.9435	43.5849	65.5179

Table 2: The χ^2_{min} , Akaike Information Criterion (AIC) and Bayesian Information Criterion (BIC) obtained for the two models for the SNIa + OHD dataset.

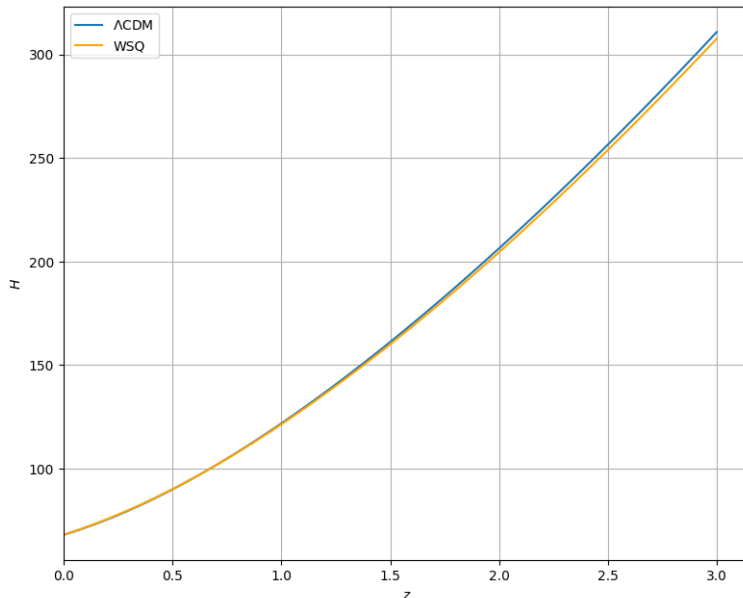


Figure 2: The evolution of Hubble parameter(H) against redshift(z) for the WSQ model and Λ CDM using the best-fit parameters for SNIa+OHD dataset.

4 Cosmographic Parameters

This section deals with studying the evolution of various cosmographic parameters to understand the background evolution of the universe as explained by the WSQ model. One such parameter of profound relevance is the Hubble parameter. The evolution of H according to the WSQ model compared to that in the Λ CDM is shown in Fig. 2. The evolution of the Hubble parameter is very similar to the Λ CDM model in the past and at present.

The evolution of the equation of state parameter ω of the scalar field ϕ is dynamical, while it is a constant in the Λ CDM with a value $= -1$ during the entire evolution of the Universe. The evolution of ω is presented in Fig. 3. It is evident that for $z > 4.43$, the scalar field together with matter contributed to the deceleration. For $z < 4.43$, $-\frac{1}{3} < \omega < -1$, showing that the scalar field started contributing to the accelerated expansion, representing a freezing model of quintessence. The present value of ω is obtained as -0.9617 .

The age of the Universe at a scale factor a can be obtained from the definition of Hubble parameter $H = \dot{a}/a$ as,

$$t_a - t_b = \int_0^a \frac{1}{aH(a)} da, \quad (24)$$

where t_a is the age of the Universe at scale factor a and t_b is the age at the moment of the big bang, which is assumed to be zero. The age of the Universe with respect to the redshift (z) is plotted in Fig. 4. The present age of the universe is obtained at $z = 0$ and the computation results in an age of 13.6

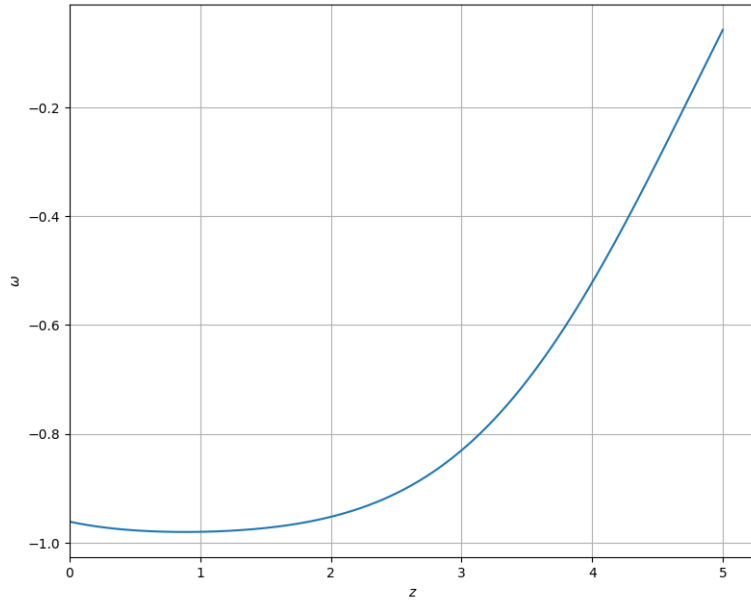


Figure 3: Evolution of the equation of state (ω) against redshift(z), plotted with the best-fit parameters obtained for SNIa+OHD dataset.

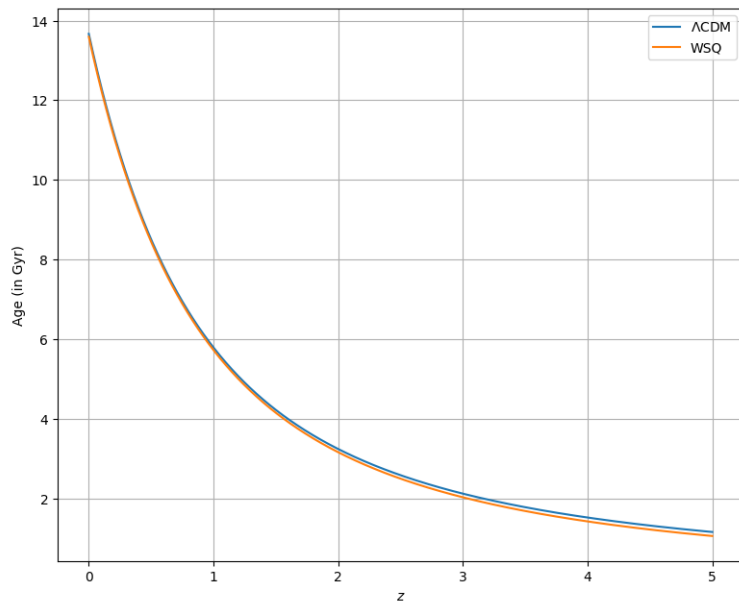


Figure 4: The age of the Universe against redshift(z) is plotted for the WSQ model and Λ CDM using the best-fit parameters obtained for the SNIa + OHD dataset.

Gyr, which is slightly less than the age obtained for the Λ CDM from the Planck data. The age of the universe inferred from CMB Planck data with Λ CDM model [15] is 13.8 Gyr. The age of the Universe computed for the Λ CDM model with the same dataset is 13.7 Gyr.

The evolution of matter and dark energy density in the WSQ model is plotted in Fig. 5. The matter energy density evolves exactly similar to the Λ CDM model, while the dark energy density or the energy density of the field slowly increases with redshift. It is clear that the dark energy dominates matter in late time, for redshift $z < 0.33$, which is in agreement with the predictions of standard Λ CDM.

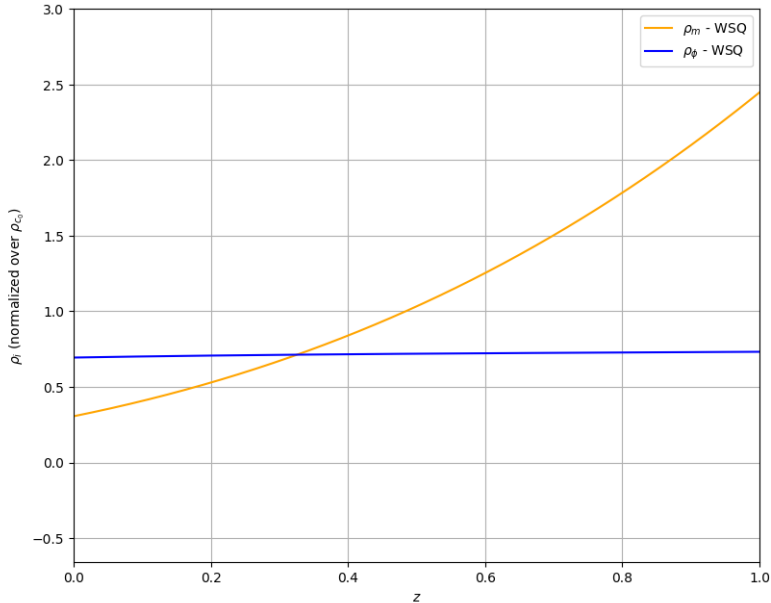


Figure 5: Evolution of matter and dark energy density in the WSQ model plotted with best-fit parameters obtained for the SNIa + OHD dataset.

The deceleration parameter q serves as an indicator to the acceleration/deceleration of the Universe in the Friedmann-Lemaitre-Robertson-Walker (FLRW) background. It is expressed as,

$$q = -1 - \frac{\dot{H}}{H^2}. \quad (25)$$

In terms of redshift, we can express Eq. (25) as,

$$q = -1 + \frac{(1+z)}{H} \frac{dH}{dz}. \quad (26)$$

A negative value for q would signify accelerated expansion of the Universe. In the WSQ model, we obtain the present deceleration parameter value of $q_0 = -0.501$, supporting the current accelerated expansion of the Universe. The redshift at which the Universe transitioned from decelerating to accelerating expansion is estimated to be $z_T = 0.662$ as compared to a value of 0.70 obtained from the Λ CDM. The WSQ model is successful in explaining the observed accelerated expansion of the Universe and the transition from decelerating to accelerating phase. The evolution of deceleration parameter with redshift is plotted in Fig. 6.

The statefinder pair (r, s) is a diagnostic tool for studying dark energy models, initially introduced by Sahni et al. in Ref. [59], where r is the jerk parameter and s is a new parameter constructed from

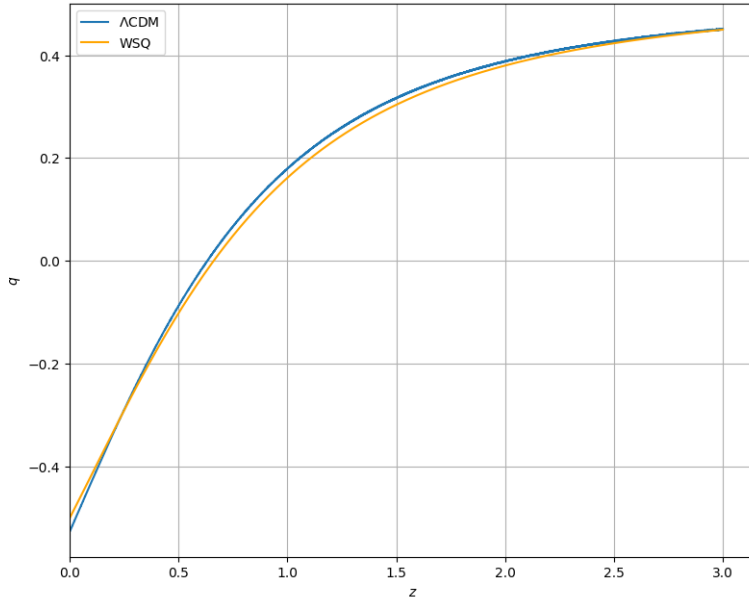


Figure 6: Evolution of deceleration parameter q with redshift z for the WSQ model and Λ CDM, plotted with best-fit parameters obtained for the SNIa+OHD dataset.

r and the deceleration parameter q . The jerk parameter is defined as [60],

$$r = \frac{1}{a} \frac{d^3 a}{dt^3} \left[\frac{1}{a} \frac{da}{dt} \right]^{-3} = \frac{\ddot{a}}{aH^3}. \quad (27)$$

We can represent r in terms of the dimensionless Hubble parameter h while introducing a new variable $N = \log_e(a)$, we obtain,

$$r = \frac{1}{2h^2} \frac{d^2 h^2}{dN^2} + \frac{3}{2h^2} \frac{dh^2}{dN} + 1. \quad (28)$$

The s parameter is defined as ,

$$s = \frac{r - 1}{3(q - 1/2)}. \quad (29)$$

On expressing q presented in Eq. (25) in terms of N and substituting in Eq. (29), we obtain

$$s = -\frac{\frac{1}{2h^2} \frac{d^2 h^2}{dN^2} + \frac{3}{2h^2} \frac{dh^2}{dN}}{\frac{3}{2h^2} \frac{dh^2}{dN} + \frac{9}{2}}. \quad (30)$$

The statefinder trajectory distinguishes the behaviour of different types of dark energy models. The trajectory is plotted in Fig. 7.

The statefinder trajectory reveals the quintessence behaviour in the present and future while the field behaved as a Chaplygin gas in the past. The present value of the statefinder diagnostic pair is obtained as $(r, s) = (0.8309, 0.0562)$, different from the Λ CDM fixed point $(1, 0)$.

5 Conclusion

In the presented work, we examined the proposed Woods Saxon quintessence model with observational constraints. We have applied MCMC methods for the Bayesian inference of the model parameters

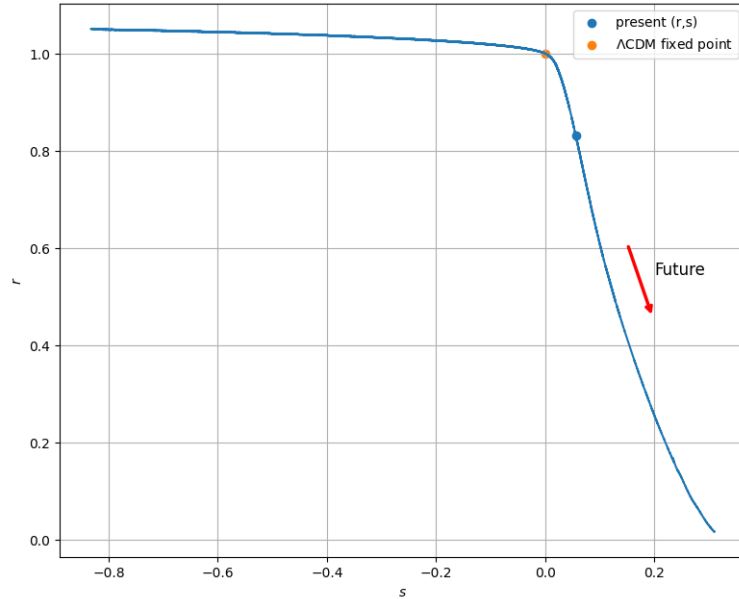


Figure 7: The statefinder trajectory is plotted using the best-fit parameters from the SNIa + OHD dataset. The fixed point of Λ CDM is also marked.

using the data combination SNIa + OHD. Our analysis shows that the model is consistent with the observational data and the obtained values of parameters are also consistent with that obtained with Λ CDM for the same dataset. The obtained best-fit values of model parameters are $H_0 = 68.10 \pm 0.74$, $\Omega_{m_0} = 0.31 \pm 0.01$ and $y_0 = 0.83 \pm 0.01$, which is in close agreement with Λ CDM predictions. The WSQ model is preferred over the Λ CDM according to χ^2_{min} and AIC, while according to the BIC criteria, the Λ CDM is slightly preferred over the WSQ model, because of the extra parameter.

The study of evolution of different cosmological parameters also revealed the consistency of the WSQ model in explaining the late-time background evolution of the Universe. The evolution of ω shows a freezing model of quintessence. Age of the Universe is estimated to be 13.6 Gyr, which is slightly less than that predicted by the Λ CDM. The present value of the deceleration parameter obtained with the WSQ model is negative, showing that the model predicts present day accelerated expansion. The Universe transitioned from decelerating to accelerating is at a redshift $z_T = 0.662$. The statefinder trajectory reveals that the field behaves as a Chaplygin gas before reaching the Λ CDM fixed point and as a quintessence after this point.

In summary, the model is consistent with the observations to good extent and can be considered as a potential alternative to the Λ CDM to explain the late phase acceleration of the Universe.

The Hubble tension is one of the most important challenges faced by modern cosmology. Our analysis shows that the Hubble parameter value obtained for the WSQ model is close to the CMB predicted value assuming the standard Λ CDM, while there exists a 3.9σ tension with the Hubble constant value obtained by the SH0ES collaboration [61]. In this work, we considered a quintessence which does not couple with ordinary matter. There are attempts in literature to alleviate the Hubble tension by introducing interaction between dark matter and the field [62]. Hence, we extend this study by introducing non-minimal coupling between matter and field as an attempt to alleviate the Hubble tension.

References

- [1] Adam G. Riess et al *Astron. J.*, vol. 116, p. 1009, 1998.
- [2] S. Perlmutter et al *Astrophys. J.*, vol. 517, p. 565, 1999.
- [3] M. Tegmark *Astrophys. J.*, vol. 514, p. L69, 1999.
- [4] D. N. Spergel et al *Astrophys. J.*, vol. 148, p. 175, 2003.
- [5] Daniel J. Eisenstein et al *Astrophys. J.*, vol. 633, p. 560, 2005.
- [6] J. Sollerman et al *Astrophys. J.*, vol. 703, p. 1374, 2009.
- [7] V. Sahni and A. Starobinsky *Int. J. Mod. Phys. D*, vol. 09, no. 04, pp. 373–443, 2000.
- [8] S. Weinberg *Rev. Mod. Phys.*, vol. 74, p. 3160, 1989.
- [9] Miguel Quartin et al *JCAP*, vol. 05, p. 007, 2008.
- [10] H. Velten, R. vom Marttens, and W. Zimdahl *Eur. Phys. J. C*, vol. 61, p. 1, 2014.
- [11] Adam G. Riess et al *Astrophys. J. Lett.*, vol. 908, p. L6, 2021.
- [12] Adam G. Riess et al *Astrophys. J.*, vol. 876, p. 85, 2019.
- [13] S. Joudaki, H. Hildebrandt, D. Traykova, N. E. Chisari, C. Heymans, A. Kannawadi, K. Kuijken, A. H. Wright, M. Asgari, T. Erben, H. Hoekstra, B. Joachimi, L. Miller, T. Tröster, and J. L. van den Busch *Astron. Astrophys.*, vol. 638, p. L1, 2020.
- [14] E. Lusso, E. Piedipalumbo, G. Risaliti, M. Paolillo, S. Bisogni, E. Nardini, and L. Amati *Astron. Astrophys.*, vol. 628, p. L4, 2019.
- [15] N. Aghanim et al *Astron. Astrophys.*, vol. 641, p. A6, 2020.
- [16] N. P. A. R. Ade *Astron. Astrophys.*, vol. 594, p. A13, 2016.
- [17] S. D. Odintsov, D. Sáez-Chillón Gómez, and G. S. Sharov *Nucl. Phys. B*, vol. 966, p. 115377, May 2021.
- [18] T. Clifton, P. G. Ferreira, A. Padilla, and C. Skordis *Phys. Rep.*, vol. 513, p. 1–189, Mar. 2012.
- [19] K. Koyama *Rep. Prog. Phys.*, vol. 79, p. 046902, 2016.
- [20] A. Silvestri, L. Pogosian, and R. V. Buniy *Phys. Rev. D*, vol. 87, p. 104015, 2013.
- [21] K. Bamba and S. D. Odintsov *New J. Phys.*, vol. 7, no. 1, pp. 220–240, 2007.
- [22] E. J. Copeland, M. Sami, and S. Tsujikawa *Int.J.Mod.Phys.D*, vol. 15, pp. 1753–1936, 2006.
- [23] S. Pan, W. Yang, E. D. Valentino, E. N. Saridakis, and S. Chakraborty *Phys. Rev. D*, vol. 100, p. 103520, 2019.
- [24] T. Karwal, M. Raveri, B. Jain, J. Khoury, and M. Trodden *Phys. Rev. D*, vol. 105, p. 063535, 2022.
- [25] R. Murgia, G. F. Abellán, and V. Poulin *Phys. Rev. D*, vol. 103, p. 063502, 2021.
- [26] C. Krishnan, E. A. Colgáin, M. Sheikh-Jabbari, and T. Yang *Phys. Rev. D*, vol. 103, p. 103509, 2021.
- [27] K. Bamba, S. Capozziello, and S. N. et al *Astrophys. Space Sci.*, vol. 342, p. 155–228, 2012.
- [28] F. Niedermann and M. S. Sloth *Phys. Rev. D*, vol. 102, p. 063527, 2020.

- [29] Ujjaini Alam et al *JCAP*, vol. 06, p. 008, 2004.
- [30] Joan Solà Peracaula et al *Europhys. Lett.*, vol. 134, p. 19001, 2021.
- [31] Ignatios Antoniadis et al *New J. Phys.*, vol. 9, p. 11, 2007.
- [32] R. R. Caldwell, R. Dave, and P. J. Steinhardt *Phys. Rev. Lett.*, vol. 80, p. 1582, 1998.
- [33] C. Armendariz-Picon, V. Mukhanov, and P. J. Steinhardt *Phys. Rev. Lett.*, vol. 85, p. 4438, 2000.
- [34] A. Kamenshchik, U. Moschella, and V. Pasquier *Phys. Lett. B*, vol. 511, no. 2, pp. 265–268, 2001.
- [35] I. Zlatev, L. Wang, and P. J. Steinhardt *Phys. Rev. Lett.*, vol. 82, p. 896, 1999.
- [36] S. Tsujikawa *Class. Quantum Grav.*, vol. 30, p. 214003, 2013.
- [37] R. R. Caldwell and E. V. Linder *Phys. Rev. Lett.*, vol. 95, p. 141301, 2005.
- [38] T. Chiba and K. Kohri *Prog.Theor.Phys.*, vol. 107, pp. 631–636, 2002.
- [39] P. Brax and J. Martin *Phys. Rev. D*, vol. 61, p. 103502, 2000.
- [40] J. F. Jesus, R. C. Santos, J. S. Alcaniz, and J. A. S. Lima *Phys. Rev. D*, vol. 78, p. 063514, 2008.
- [41] F. Perrotta, C. Baccigalupi, and S. Matarrese *Phys. Rev. D*, vol. 61, p. 023507, 1999.
- [42] L. P. Chimento, A. S. Jakubi, and D. Pavón *Phys. Rev. D*, vol. 62, p. 063508, 2000.
- [43] I. Affleck, M. Dine, and N. Seiberg *Nucl. Phys. B.*, vol. 256, pp. 557–599, 1985.
- [44] C. T. Hill and G. G. Ross *Phys. Lett. B.*, vol. 203, pp. 125–131, 1988.
- [45] Y. Nomura, T. Watari, and T. Yanagida *Phys. Lett. B.*, vol. 484, pp. 103–111, 2000.
- [46] J. E. Kim and H.-P. Nilles *Phys. Lett. B.*, vol. 553, pp. 1–6, 2003.
- [47] Y. S. Sudhakar Panda and S. P. Trivedi *Phys. Rev. D.*, vol. 83, p. 083506, 2011.
- [48] C. Armendariz-Picon, V. Mukhanov, and P. J. Steinhardt *Phys. Rev. D*, vol. 63, p. 103510, 2001.
- [49] M. Malquarti, E. J. Copeland, A. R. Liddle, and M. Trodden *Phys. Rev. D*, vol. 67, p. 123503, 2003.
- [50] A. D. Rendall *Class. Quantum Grav.*, vol. 23, p. 1557, 2006.
- [51] C. Armendariz-Picon and E. A. Lim *JCAP*, vol. 08, p. 007, 2005.
- [52] S. M. Carroll *Phys. Rev. Lett.*, vol. 81, p. 3067, 1998.
- [53] R. Trotta *Contemp. Phys.*, vol. 49(2), pp. 71–104, 2008.
- [54] J. Singh, H. Balhara, and P. S. Shaily *Astron. Comp.*, vol. 46, p. 100795, 2024.
- [55] Dan Scolnic et al *Astrophys. J.*, vol. 938, p. 113, 2022.
- [56] Dillon Brout et al *Astrophys. J.*, vol. 938, p. 110, 2022.
- [57] Daniel Foreman-Mackey et al *PASP*, vol. 125, no. 306, 2013.
- [58] J. Goodman and J. Weare *Commun. Appl. Math. Comput.*, vol. 5, pp. 65–80, 2010.
- [59] V. Sahni, T. Saini, A. Starobinsky, and U. Alam *JETP Lett.*, vol. 77, pp. 201–206, 2003.
- [60] M. Visser *Class. Quantum Grav.*, vol. 21, p. 2603, 2004.
- [61] A. G. Riess, W. Yuan, L. M. Macri, D. Scolnic, D. Brout, S. Casertano, D. O. Jones, Y. Murakami, G. S. Anand, L. Breuval, et al. *Astrophys. J. Lett.*, vol. 934, no. 1, p. L7, 2022.
- [62] B. J. Barros, L. Amendola, T. Barreiro, and N. J. Nunes *JCAP*, vol. 2019, p. 007, jan 2019.